

Low-Temperature Spark Plasma Sintering of Pure Nano WC Powder

Salvatore Grasso,[‡] Johannes Poetschke,^{§,†} Volkmar Richter,[§] Giovanni Maizza,[¶]
Yoshio Sakka,^{*,||} and Michael J. Reece^{*,‡}

[‡]School of Engineering & Materials Science and Nanoforce Technology Ltd., Queen Mary University of London,
Mile End Road, London E1 4NS, UK

[§]Fraunhofer Institute for Ceramic Technologies and Systems, Winterbergstraße 28, Dresden 01277, Germany

[¶]Dipartimento di Scienza dei Materiali ed Ingegneria Chimica, Politecnico di Torino, Corso Duca degli Abruzzi 24,
Torino I-10129, Italy

^{||}Advanced Materials Processing Unit, National Institute for Materials Science, 1-2-1 Sengen, Tsukuba, 305-0047, Ibaraki, Japan

For the first time we have demonstrated the densification of high-purity nanostructured ($d_{\text{avg}} \approx 60$ nm) tungsten carbide by High Pressure Spark Plasma Sintering (HPSPS) in the unusually low temperature range of 1200°C–1400°C. The high-pressure sintering (i.e., 300 MPa) produced dense material at a temperature as low as 1400°C. In comparison with more conventional sintering techniques, such as SPS (80 MPa) or hot isostatic pressing, HPSPS lowered the temperature required for full densification by 400°C–500°C. High Pressure Spark Plasma Sintering, even in absence of any sintering aid or grain growth inhibitor, retained a very fine microstructure resulting in a significant improvement in both hardness (2721 HV₁₀) and fracture toughness (7.2 MPa m^{1/2}).

I. Introduction

DURING the past two decades, wear resistance, hardness, and toughness of cemented carbides have been increased by grain-size refinement.¹ To achieve complete densification of the starting WC powders and a fine-grained microstructure, small amounts (≈ 1 wt%) of grain growth inhibitors and binder metals are typically employed. However, metallic binders usually result in reduced hardness and corrosion/oxidation resistance.² Whereas traditional hardmetals are densified via liquid phase sintering at around 1350°C,³ so called binderless hardmetals require sintering temperatures between 1700°C and 2000°C.

Traditionally, hot pressing or hot isostatic pressing (HIP) have been mainly used to manufacture fully dense WC ceramics.⁴ More recently SPS combining high heating rates, electric field effects has been demonstrated as an effective technique to limit grain growth and to produce dense samples with submicrometric grain size.⁵ To achieve fully dense binderless WC by SPS, while maintaining a submicrometric grain size, different grain growth inhibitors are typically added.⁶ Kawakami et al.⁷ have shown that in the case of cemented carbides the effect of grain growth inhibitors is related to their dissolution in the liquid phase, and that their

efficiency in grain-boundary pinning decreases in the order VC > Cr₃C₂ > TiC > TaC.

The objectives of this research study are as follows: (1) to overcome the limitation of existing sintering techniques in terms of sintering pressure and to promote full densification at low temperature; (2) investigate mechanism involved in high-pressure nano-sintering; (3) achieve pore free nanostructured WC with improved hardness and toughness in the absence of any sintering aid.

II. Experimental Procedure

The starting powders for the experiments were pure WC powder made by H. C. Starck with a grain size of 119 nm (D_{BET})/420 nm (D_{FSSS}) designated as powder WC120. The nano-powder WC 60 was achieved by milling for 8 h at 700 rpm, under nitrogen in n-Heptan as a solvent and WC-6Co milling balls. After milling the powders were dried using a vacuum dryer and sieve granulated.

The powders were sintered using an SPS furnace (FCT HP D 20; FCT Systeme GmbH, Rauenstein, Germany) under vacuum (5 Pa). Typically, a HPSPS die set is made of either SiC or WC. Due to the sintering temperature exceeding 1100°C, SiC rather than WC was used as the material for the punches. The high-pressure device is sketched in Fig. 1. This device allows the application of a pressure even above 500 MPa on a sample of 10 mm in diameter and ~ 4 mm thickness. In a typical sintering experiment, 5 g of WC powder was poured into the die. The device is composed of an outer and an inner graphite die, and the powder is pressed between the two SiC punches between two SiC disks.⁸ As shown in Fig. 1, the punch ($\Phi 10$ h 15 mm) and disk ($\Phi 30$ h 20 mm) were made of SiC and the remaining parts of the device was made up of graphite. The inner and outer diameters of the internal mold were 10 and 30 mm, respectively, its height was 30 mm. The inner and outer diameters of the external mold were 30 and 60 mm, respectively, its height was 100 mm. The temperature was accurately controlled using a pyrometer focused on the die surface of the inner die (i.e., 1 cm away from the sample). The powder was heated from room temperature up to the sintering temperature at 50°C/min. During dwelling, the temperature measured by the side pyrometer was about 200°C higher than the one measured by the top pyrometer.

By increasing the sintering temperature, the dwelling time was progressively decreased from 20 to 10 minutes. Pressure was linearly raised during heating reaching 300 MPa at 1200°C. The milled powder was sintered at 1200°C–1400°C.

S. Huang—contributing editor

Manuscript No. 32506. Received December 19, 2012; approved April 2, 2013.

*Member, The American Ceramic Society.

[†]Author to whom correspondence should be addressed: e-mail: johannes.poetschke@ikts.fraunhofer.de

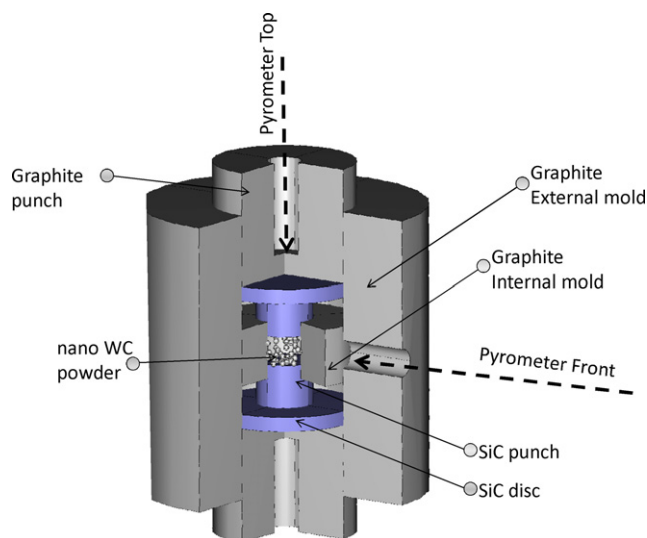


Fig. 1. Schematic of high-pressure spark plasma sintering (HPSPS) device. The pure WC powder was compressed between two SiC punches pushed by the SiC protective disks. The temperature was controlled by a pyrometer pointed on the inner die surface (i.e., 1 cm far from the sample). The top Pyrometer was also employed to probe temperature (4 cm far from the sample).

To account the effect of milling on the sintering behavior, the as-received unmilled powder was sintered at 1350°C. The samples were named according to the particle size and sintering temperature.

The density was determined according to DIN ISO 3369. Porosity was measured according to DIN ISO 4505 using an optical microscope with a magnification of 100 and 500 times. The microstructure was observed using a field-emission scanning electron microscope (FESEM) LEO 982 (Carl Zeiss SMT AG, Oberkochen, Germany). The Vickers hardness (HV10) of samples was measured according to DIN ISO 3878 with a load of 98.1N. The fracture toughness (K_{IC}) was calculated from the Vickers indentation crack length using the Shetty equation.⁹ The given relative density was estimated using a theoretical density of WC for 15.67 g/cm³.

The XRD measurements were performed using a Bruker D8 diffractometer (Billerica, MA). The diffractometer used the Bragg-Brentano geometry and CuK α ($\lambda = 0.15418$ nm) radiation 2 θ range was 20°–100°. A Rietveld refinement was done using the computer program TOPAS (DIFFRAC.SUITE TOPAS, from Bruker) to obtain detailed information on crystallite size and of the phase composition. BET measurements were done using ASAP 2010 from Micromeritics Instrument Corporation, (Norcross, GA) and a five-point analysis. To determine the amount of Co introduced by milling the powder with WC-Co balls, samples of milled and unmilled powders were dissolved in 0.1 mol/l HCl acid for 24 h. The Co concentration in the solutions was determined by means of ICP-OES. Carbon measurements were done using a gas analyzer WC600 from LECO Corporation (St. Joseph, MI).

III. Results and Discussion

The average particle size measured using BET-surface analysis before and after milling were 120 and 60 nm, respectively. Figure 2 shows the FESEM images of (a) as-received WC powder and (b) after ball-milling. As also confirmed by SEM images, the ball milling reduced dramatically the particle size. The powder as-received shows a bimodal particle size distribution [Fig. 2(a)], with rounded particles with size below 200 nm coexisting with larger ones. After ball-milling the particles became finer, but the bimodal particle distribution is maintained as confirmed in Fig. 2(b).

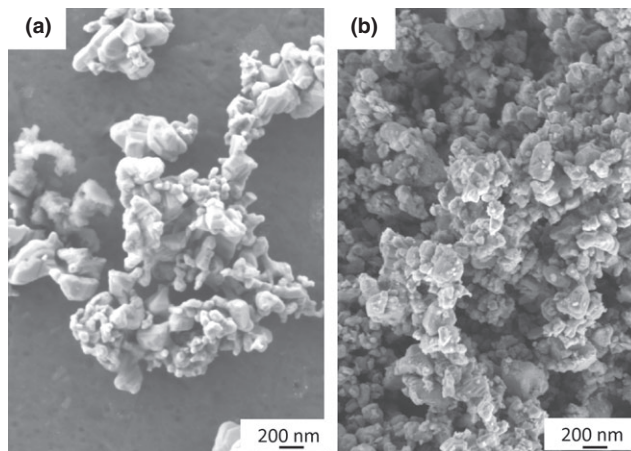


Fig. 2. Field emission scanning electron microscope (FESEM) SEM image of nanostructured WC powder (a) before and (b) after milling.

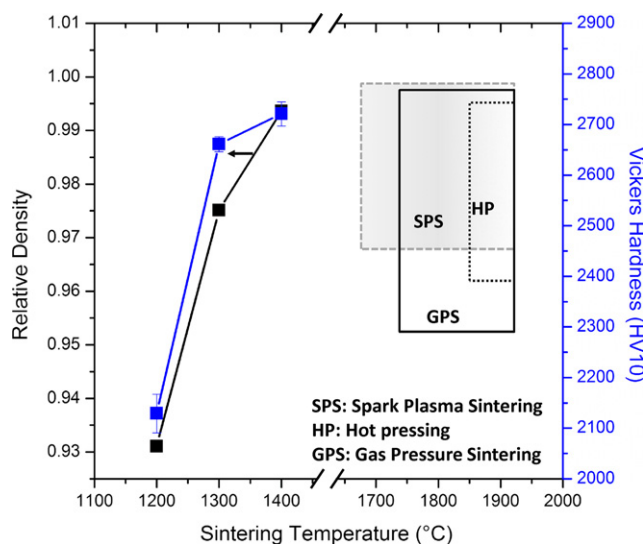


Fig. 3. Right-hand side, plot of density and hardness for ball-milled nanostructured WC powder sintered by high-pressure spark plasma sintering under 300 MPa compressive stress. The dwell time for 1200°C–1400°C was decreased from 20 to 5 min. Left side, typical densification of parameters for conventional spark plasma sintering (SPS) (i.e., 60 MPa), Gas Pressure Sintering and Hot Pressing for ultrafine WC powder are also shown. Theoretical density of WC is assumed as 15.67 g/cm³.

Figure 3 shows the density and Vickers hardness for the samples sintered by high-pressure SPS. In the same figure, the typical sintering temperature to achieve nearly fully dense samples starting from ultrafine ($d_{avg} \approx 103$ nm) WC (containing Cr₃C₂ grain growth inhibitor, commercially known as WC02N ALMT Corp, Japan) with different sintering techniques⁵ are also shown. Figure 3 clearly illustrates the difference in terms of sintering temperature to achieve high density in the present study in relation with the state of the art. As reported in previous studies, to achieve dense WC material, temperatures as high as 2000°C¹⁰ were needed in the case of conventional vacuum sintering without external pressure, while temperatures around 1750°C–1900°C^{4,5} were necessary in the case of pressure sintering techniques such as hot pressing or hot isostatic pressing. In case of sintering above 1700°C (left side Fig. 3), to maintain fine microstructure corresponding to ultrafine and dense WC with hardness/toughness exceeding 2500 HV10/4.5 MPa m^{1/2}, grain growth inhibitors are used.^{6,11}

Using the SPS technique, temperatures as low as 1600°C were reported to produce dense samples.¹² Recently, Grasso

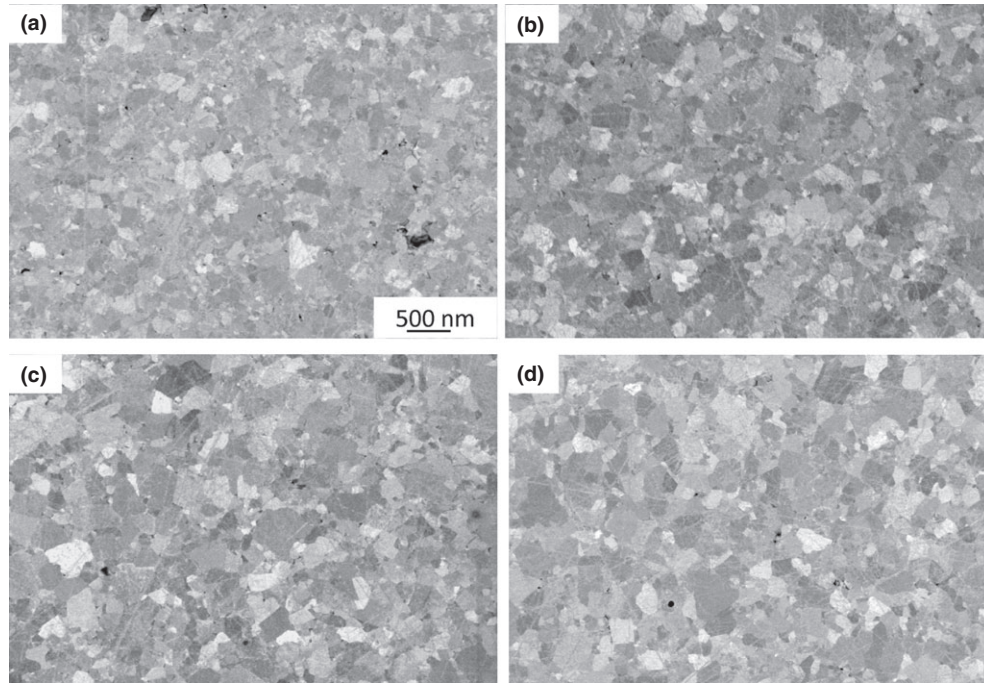


Fig. 4. Backscattered electron images of ball milled nano WC 60 powder sintered by high-pressure spark plasma sintering (HPSPS) at (a) 1200, (b) 1300, (c) 1400, and (d) WC 120 sintered at 1350°C.

et al.¹¹ clarified the temperature distribution inside an SPS punch die assembly. Using a combined experimental-numerical methodology suggests that dense ultrafine WC sample can be obtained at sintering temperatures exceeding 1750°C under 80 MPa compressive pressure. Thus, the sintering temperature referred to the die surface as done in previous research¹² is inappropriate to describe the actual sintering temperature. Huang et al.¹³ used more accurate temperature measurement based on two SPS pyrometer configurations. They found that fully dense ultrafine WC samples could be obtained at temperature exceeding 1800°C.

In this research study, the preferential current distribution inside the graphite mold resulting from the poor electrical conductivity of SiC (Fig. 1), did not result in presence of any significant thermal gradient,¹¹ thus, it is correct to assume that the inner die temperature is really close to that of the sample ($\pm 10^\circ\text{C}$).

The cobalt contamination resulting from the intensive ball milling was minimal, in fact according to the ICP-OES analysis Co content of milled powder was slightly increased from 0.01 to 0.11 wt%. Thus, the effectiveness of HPSPS in achieving nearly fully dense samples at low temperature cannot be attributed to the cobalt contamination. The densification of the unmilled sample WC120-1350 is fully comparable to that of the milled powder WC60 at 1300°C.

As detailed in Table I, by employing HPSPS it was possible to achieve density as high as 97.5% at only 1300°C. Thus, the temperature difference to achieve near full densification (>97%) between high-pressure and conventional

SPS^{5,11,13} of about 400°C can be attributed primarily to effects related to high-pressure sintering. Most of the shrinkage (more than 90%) occurred during the pressure application (i.e., 1200°C, 300 MPa). To help understanding the sintering behavior under high pressure, we may recall the concept of superplasticity in nanograined ceramics. For example, in the case of WC plastic mechanism under stress of 300 MPa might be activated starting from 1200°C (i.e., $0.5 T_m$ which corresponds to 1500 K) as reported by Jimenez-Melendo et al. in the case of stabilized zirconia.¹⁴

As shown in Table I and Fig. 3, at 1400°C the density nearly reached the theoretical density of 15.67 g/cm³ resulting in a relative density of 99.3%. The best combination of hardness and toughness was achieved for the sample sintered at 1400°C for 10 min with hardness and toughness as high as 2720 (HV10) and 7.2 (MPa m^{1/2}). The hardness increases with relative density (Fig. 3). Samples sintered above 1200°C showed comparable toughness and hardness with average values of 2650 and 6.9 MPa m^{1/2}.

As confirmed by XRD, ball-milled powder consisted of single phase WC, with a crystallite size of 40 nm. For the samples sintered at 1200°C and 1300°C the crystallite size calculated using the Rietveld-analysis were 84 and 136 nm. For the samples sintered at 1400°C there was a good match between the XRD (295 nm) estimation and SEM analyzing (310 nm), in both cases the crystallite size was ~300 nm. Despite the low sintering temperature, WC showed a remarkable tendency to grain growth. This might be attributed to grain coalesce effect promoted by high pressure as reported

Table I. List of Sample Processing Conditions and Measured Properties Including Relative Density, Hardness, Indentation Fracture Toughness, Average Crystallite Size By Rietveld Refinement, and Carbon content

Sample details	Relative density	Hardness [HV10]	Fracture toughness [MPa m ^{1/2}]	Crystallite size XRD [nm]	W ₂ C content [Wt%]	Carbon Content [Wt%]
WC60-1200-20 min	93.1	2129 \pm 38	5.9	84	0	5.90
WC60-1300-20 min	97.5	2661 \pm 15	6.9	136	2.4	5.93
WC60-1400-10 min	99.3	2721 \pm 24	7.2	295	4.5	5.96
WC120-1350-20 min	97.7	2710 \pm 18	6.8	175	3.6	6.01

in Ref. 15. For samples sintered at 1400°C, it was difficult to resolve the crystallites by backscattered electron imaging, and SEM images overestimated the crystallite sizes.

The carbon content was affected by milling conditions, sintering temperature, and sintering time. For example the WC60-1300-20 has a carbon content of 5.93 wt%, which is below the 6.01 wt% of WC120-1350-20. Such a difference might be due to undesired oxidation that occurred during the powder milling process. As confirmed by the samples sintered in the range 1200°C–1400°C, the ascending level of carbon might be attributed to the increased sintering temperature, thus carbon might have been transferred by the graphite foil surrounding the sample employed for the SPS processing. Pure WC contains 6.13 wt% carbon. Difference with nominal compositing, as shown in Table I, can be attributed to the presence of carbon deficiency phases.

Table I also lists the weight fraction of the W_2C phase for samples sintered in the temperature range 1200°C–1400°C. The presence of this phase is due to the undesired surface oxidation of the nanometric powders.¹⁶ With increasing sintering temperature from 1200°C to 1400°C the samples showed a growing content of the W_2C phase. Parts of the under stoichiometric WC as well as remaining WO_3 reduced slowly decompose to W_2C . However, because diffusion of C and W is temperature controlled the amount of formed W_2C increases slowly with increasing sintering temperature. Thus, the pore-free and dense microstructure at all temperatures and the increase in absolute density as well of the measured properties (HV10, K_{IC}) over the temperature is most likely due to a carburization processes of W during sintering.

In comparison with previously published data on the densification of same powder as employed in this study (i.e., WC 120 from H. C. Starck) processed by conventional SPS, the newly developed HPSPS allowed the following: (1) slightly higher hardness toughness of 2720 HV10 and 7.2 MPa $m^{1/2}$ against 2600 HV10 and 4.4 MPa $m^{1/2}$ ¹³; (2) a lowering in the sintering temperature by 400°C–500°C while still achieving samples with density well above 99%; (3) avoiding the use of both sintering aids and grain growth inhibitors.⁶

IV. Conclusions

The role of high pressure on the spark plasma sintering of nanostructured tungsten carbide was investigated for the first time. The high pressure enhances the densification at very low temperature. Pore-free high-purity WC samples were achieved at a temperature as low as 1400°C. Samples sintered at 1200°C were 93% dense with an average crystallite size of 84 nm. In comparison with previous studies conducted on

the same powder by conventional SPS, the newly developed HPSPS, even in absence of any grain growth inhibitor, allowed to lower the sintering temperature by 400°C–600°C while still achieving a pore-free microstructure with a relative density well above 99% and improvements in both hardness and toughness.

References

- ¹Z. Z. Fang, X. Wang, T. Ryu, K. S. Hwang, and H.Y. Sohn, "Synthesis, Sintering, and Mechanical Properties of Nanocrystalline Cemented Tungsten Carbide – A review," *Int. J. Refract Metal Hard Mater.*, **27**, 288–99 (2009).
- ²H. Suzuki, *Cemented Carbide and Sintered Hard Materials*. Japan Maruzen Publishing Company, Tokyo, pp. 262–73, 1986.
- ³V. Richter and M. Ruthendorf, "On Hardness and Toughness of Ultrafine and Nanocrystalline Hard Materials," *Int. J. Refract Metal Hard Mater.*, **17**, 141–52 (1999).
- ⁴Y. Kanemitsu, T. Nishimura, H. Yoshino, K. Takao, and Y. Masumoto, "Effect of Hot Isostatic Pressing on Binderless Cemented Carbide," *Refract Metal Hard Mater.*, **1**, 66–8 (1982).
- ⁵V. Richter, R. Holke, and M. Ruthendorf, "Properties of Binderless Hard-metal Densified by SinterHIP, Hot Pressing and SPS"; pp. 573–7 in Proceedings of the European Congress and Exhibition on Powder Metallurgy (EURO PM), EPMA, Shrewsbury, UK, 2004.
- ⁶J. Poetschke, V. Richter, and R. Holke, "Influence and Effectivity of VC and Cr_3C_2 Grain Growth Inhibitors on Sintering of Binderless Tungsten Carbide," *Int. J. Refract Metal Hard Mater.*, **31**, 218–23 (2012).
- ⁷M. Kawakami, O. Terada, and K. Hayashi, "HRTEM Microstructure and Segregation Amount of Dopants at WC/Co Interfaces in TiC and TaC Monodoped WC-Co Submicro-grained Hardmetals," *J. Jpn Soc. Powder Powder Metall.*, **53**, 166–71 (2006).
- ⁸S. Grasso, B. N. Kim, C. Hu, G. Maizza, and Y. Sakka, "Highly Transparent Pure Alumina Fabricated by High Pressure Spark Plasma Sintering," *J. Am. Ceram. Soc.*, **93**, 2460–2 (2010).
- ⁹D. K. Shetty, I. G. Wright, N. Mincer, and A. H. Clauer, "Indentation Fracture of WC–Co Cermets," *J. Mater. Sci.*, **5**, 1873–82 (1985).
- ¹⁰T. Li, Q. Li, J. Y. H. Fu, P. C. Yu, L. Lu, and C. C. Wu, "Effects of AGG on Fracture Toughness of Tungsten Carbide," *Mater. Sci. Eng.*, **445**, 587–92 (2007).
- ¹¹S. Grasso, Y. Sakka, G. Maizza, and C. Hu, "Pressure Effect on the Homogeneity of Spark Plasma-Sintered Tungsten Carbide Powder," *J. Am. Ceram. Soc.*, **92**, 2418–21 (2009).
- ¹²J. Zhao, T. Holland, C. Unuvar, and Z. A. Munir, "Spark Plasma Sintering of Nanometric Tungsten Carbide," *Int. J. Refract Metal Hard Mater.*, **27**, 130–9 (2009).
- ¹³S. G. Huang, K. Vanmeensel, O. Van der Biest, and J. Vleugels, "Binderless WC and WC–VC Materials Obtained by Pulsed Electric Current Sintering," *Int. J. Refract Metal Hard Mater.*, **26**, 41–7 (2008).
- ¹⁴M. Jimenez-Melendo, A. Dominguez-Rodriguez, and A. Brovo-Leon, "Superplastic Flow of Fine-Grained-Yttria-Stabilized Zirconia Polycrystals: Constitutive Equation and Deformation Mechanisms," *J. Am. Ceram. Soc.*, **81**, 2761–76 (1998).
- ¹⁵B. Kim, K. Hiraga, S. Grasso, K. Morita, H. Yoshida, H. Zhang, and Y. Sakka, "High-pressure Spark Plasma Sintering of MgO-doped Transparent Alumina," *J. Ceram. Soc. Jpn.*, **120**, 116–8 (2012).
- ¹⁶I. S. Cha and H. H. Soon, "Microstructures of Binderless Tungsten Carbides Sintered by Spark Plasma Sintering Process," *Mater. Sci. Eng., A*, **356**, 381–9 (2003). □